

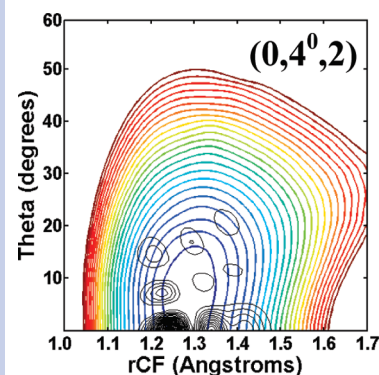
Theoretical and Experimental Spectroscopy of the S_2 State of CHF and CDF: Dynamically Weighted Multireference Configuration Interaction Calculations for High-Lying Electronic States

Richard Dawes,^{*,†} Ahren W. Jasper,[†] Chong Tao,[‡] Craig Richmond,[§] Calvin Mukarakate,[‡] Scott H. Kable,[§] and Scott A. Reid^{*,‡}

[†]Combustion Research Facility, Sandia National Laboratories, P.O. Box 969, Livermore, California 94551, [‡]Department of Chemistry, Marquette University, Milwaukee, Wisconsin 53201-1881, and [§]School of Chemistry, University of Sydney, NSW 2006, Australia

ABSTRACT Dynamically adjusting the weights in state-averaged multiconfigurational self-consistent field (SA-MCSCF) calculations using an energy-dependent functional allows the electronic wave function to smoothly evolve across the potential energy surface (PES) and correctly preserves differing asymptotic electronic-state degeneracy patterns. We have developed a generalized dynamic weighting (GDW) method to treat high-lying electronic states. To test the method, a global PES was constructed for the S_2 (\tilde{B}) state of CHF (CDF), which lies nearly 31000 cm^{-1} above the minimum of the ground state. The GDW method was used to produce SA-MCSCF reference states for subsequent multireference configuration interaction (MRCI) calculations, whose Davidson-corrected energies were extrapolated to the complete basis set limit. Quantum mechanical vibrational energy calculations for CDF were performed using the fitted PES, and the predicted energy levels are in excellent agreement with an extensive set of experimentally determined (optical–optical double resonance) levels, with a mean unsigned error of only 12 cm^{-1} .

SECTION Dynamics, Clusters, Excited States



Quantitative theoretical spectroscopy for small systems in ground electronic states is well-established.^{1–4} The errors associated with solving for the vibrational energy levels are typically small, and the overall error in the computed energy levels is primarily determined by the quality of the potential energy surface (PES). High-quality PESs may be obtained by fitting high-level ab initio data to analytic functional forms, with additional refinements based on experimental data sometimes required.^{5,6} The interpolative moving least-squares (IMLS) method accurately and efficiently interpolates a dynamically grown set of ab initio data with a negligible fitting error, thus allowing for a direct assessment of the dynamical accuracy of the underlying electronic structure method.^{7–9} Previously, vibrational energy-level calculations for $^1\text{CH}_2$ and HCN in their ground electronic states were reported for several ab initio methods using IMLS, where the fitting error was shown to be less than 1 cm^{-1} .⁹ The automated IMLS PES generator used in the present study runs in parallel, interfaces with ab initio electronic structure codes, and produces analytic fitted surfaces suitable for efficient use in spectroscopy and other dynamics applications.

Calculating accurate global PESs for excited electronic states is much more challenging.¹⁰ Multireference configuration interaction (MRCI) calculations can be accurate, but they are

not straightforward when the character and/or number of energetically relevant electronic states changes throughout the configuration range of interest.

The ab initio method of dynamically adjusting the relative weights in a state-averaged multiconfigurational self-consistent field calculation (DW-SA-MCSCF) was introduced recently by Deskevich et al. and has been implemented in the Molpro program suite.^{11,12} DW-SA-MCSCF produces a balanced description of the orbitals, smoothly evolving the wave function with respect to varying coordinates (for example, along a reaction path), thus correctly preserving differing asymptotic electronic-state degeneracy patterns. The DW scheme overcomes problems with convergence and discontinuities that can plague fixed weight calculations in certain regions of the PES, particularly when high-lying valence and Rydberg states form avoided crossings with one or more states of interest. For quantitative studies, post-MCSCF methods such as MRCI are required, and DW-MRCI denotes the use of DW-SA-MCSCF orbitals in a subsequent MRCI calculation.

Received Date: December 8, 2009

Accepted Date: January 11, 2010

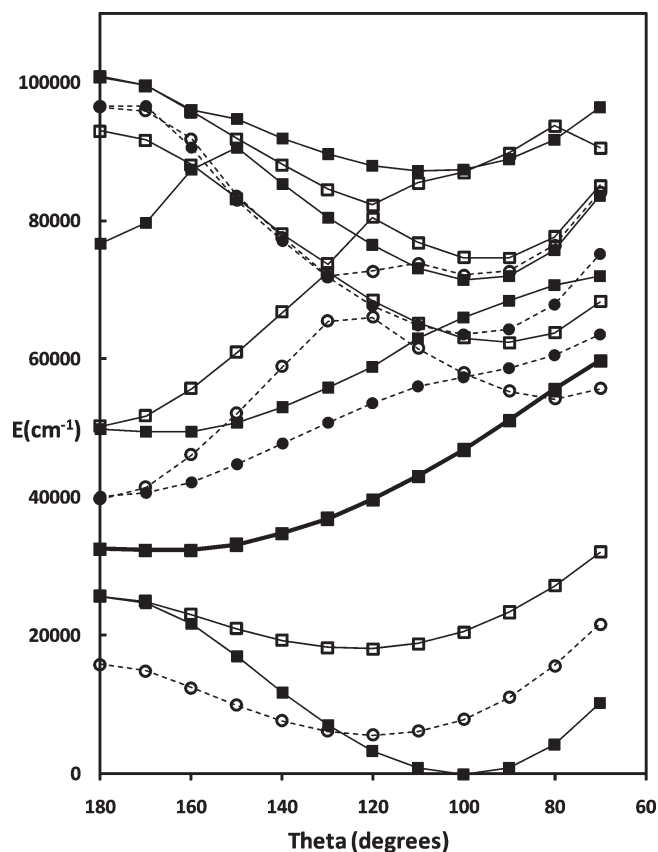


Figure 1. Calculated bend potential curves (GDW-MRCI+Q/aug-cc-pVQZ) for the lowest five $1A'$ (filled squares) and four $1A''$ (open squares) singlet states (solid lines). The \bar{B} state ($2^1A'$) of interest is highlighted with a thicker line. The lowest five triplet states are shown with dashed lines ($1-2^5A'$, filled circles, and $1-3^5A''$, open circles). All 14 states were computed simultaneously using the GDW scheme focused on the \bar{B} state and an active space of 8 electrons in 8 a' and 2 a'' orbitals. The CH and CF bond lengths were fixed at 1.07 and 1.40 Å, respectively.

A state-averaged MCSCF calculation minimizes the weighted average energy \bar{E} of two or more electronic states with respect to the molecular orbitals and the configuration expansion, where

$$\bar{E} = \sum_{i=0}^n \frac{w_i}{W} E_i \quad (1)$$

E_i and w_i are the energy and weight of the i th state, and

$$W = \sum_{i=0}^n w_i$$

In many applications, the weights are fixed (e.g., $w_i = 1$).

In the DW scheme,¹¹ the weights are determined self-consistently using an energy-dependent functional

$$w_i = \cosh^2(\Delta E_{i0}/\beta) \quad (2)$$

where $\Delta E_{i0} = E_i - E_0$ and β is a parameter ($\beta = 3.0$ eV was used in this study). The ground state always receives the largest weight, excited states receive smaller weights that depend on the difference between their energies and that of

the ground state, and degenerate states receive equal weighting. High-lying states may receive very little weight and may not be well-described as most of the variational effort is directed toward the ground and low-lying states.

We have generalized the DW scheme (denoting our method GDW) to place maximum weight on any particular state (j) of interest, that is

$$w_i = \cosh^2(\Delta E_{ij}/\beta) \quad (3)$$

where $\Delta E_{ij} = |E_i - E_j|$. The other algorithmic details described by Deskevich et al. were retained in our procedure.¹¹

There has been considerable interest in carbenes over the years from both theorists and experimentalists, including the well-known singlet–triplet gap in methylene as well as the Renner–Teller (RT) pairing of the two lowest singlet states.^{13–15} RT and spin–orbit (SO) coupling complicate the spectroscopy of the low-lying states in these systems, while complete vibrational level progressions for high-lying states have not been reported. We have recorded an extensive set of rovibrational progressions for the S_2 ($\bar{B} 2^1A'$) state of both the CHF and CDF systems, and the present Letter focuses on the CDF set of results. The \bar{B} state is not RT-paired and is energetically well-separated from any triplet states (see Figure 1).

All of the \bar{B} state vibrational levels (including the zero-point level) are predissociated (the origin of the \bar{B} state lies >6000 cm^{-1} above the $\text{H} + \text{CF}$ asymptote) and exhibit lifetime broadening. For CDF, the line widths range from 0.3 to 5.0 cm^{-1} and are roughly energy-dependent (increasing with energy). The spectrum for the CHF isotopomer is complicated by a strong CF-stretch–bend resonance, and the spectrum is further complicated by much stronger line broadening (>35 cm^{-1} for some levels) that does not follow a simple energy dependence. For these reasons and for the purpose of testing the GDW ab initio scheme, we confine the present analysis to the spectrum of CDF, where the exclusive consideration of the \bar{B} state is expected to provide an accurate description. Elucidating the mechanism responsible for line broadening and fully characterizing CHF is an avenue for future research.

The present set of experimentally well-characterized vibrational energy levels on a high-lying electronic state provides an excellent test of the accuracy of the GDW-MRCI method. The calculated vibrational energy levels are sensitive tests of the accuracy of the PES, and this in turn is a direct measure of the accuracy of the ab initio method when using the IMLS approach.

We implemented the GDW scheme (eq 3), testing various numbers of states and orbital active spaces, including as many as 24 singlet states (12 A' and 12 A'') with a full-valence active space. A nine state (5 A' and 4 A'') GDW description with an active space of eight electrons in eight a' and two a'' orbitals was found to provide a good description of the \bar{B} state and other lower-energy states in the fitted coordinate ranges. This choice of active space excludes dominant configurations from some higher-energy states but produces robust convergence in the electronic structure calculations and preserves numerically exact degeneracies for RT pairs at linear geometries (see Figure 1). Use of a full-valence active space adds three

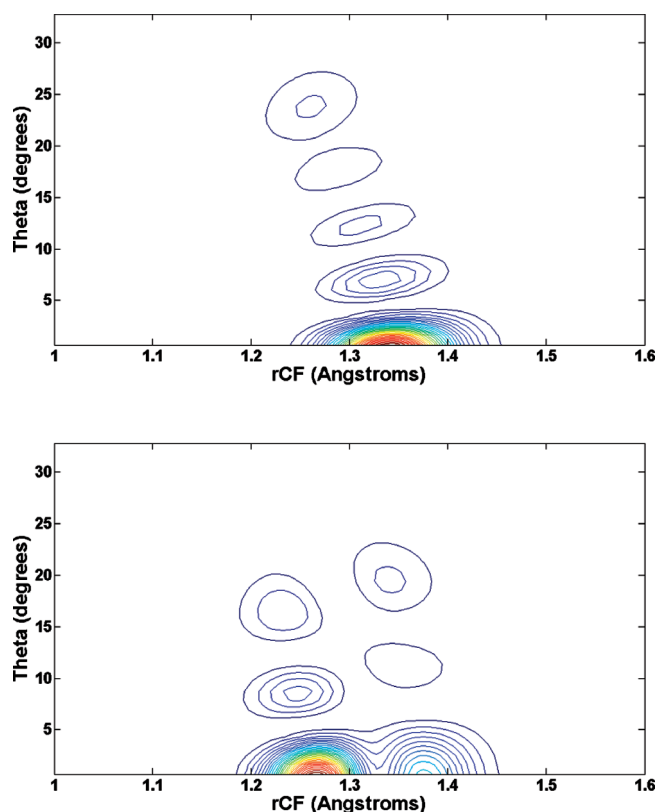


Figure 2. Examples of 2D probability density plots used to assign calculated levels (with the third Jacobi coordinate integrated out). Plots are of the $(0,8^0,0)$ level (upper) and $(0,4^0,1)$ level (lower).

additional high-lying singlet states (two A' and one A'' states) within the energy range shown in Figure 1.

The IMLS code used to generate the PES was directly interfaced with the Molpro program package.¹² In the ab initio calculations, the GDW-SA-MCSCF method was used to produce reference states for subsequent Davidson-corrected MRCI calculations (the 2s orbitals were also correlated in the MRCI calculation). Energies calculated with correlation-consistent augmented triple- and quadruple- ζ basis sets (aug-cc-pVTZ, aug-cc-pVQZ) were extrapolated to the complete basis set (CBS) limit using the Γ^{-3} formula.¹⁶ The IMLS code was run in parallel (20 processes) and terminated once a total of 2157 automatically generated ab initio energy data points were included in the PES. This is more data than is necessary to obtain a good fit for a three atom system,⁹ but a generous number were computed since the ab initio cost was not prohibitive.

Inspection of some of the ab initio calculations revealed that some of the highest-energy states received negligible weights over much of the configuration space, while the ground state received small weights ($w_0 = \sim 0.05$) in some regions. For comparison, two additional PESs (for a total of three) were also generated using different ab initio weighting strategies. The second was a nine state (5 A' and 4 A'') calculation with fixed and equal weights. The third strategy tested was a 24 state calculation with equal weights for the 1 A' , 2 A' , and 1 A'' states, with the weights for the higher-energy states determined by the GDW scheme. This third scheme

Table 1. Calculated and Experimental Frequencies for the $J = 0$ Band Origins of the \tilde{B} State of CDF (cm^{-1})^a

level	EXPT (width)	GDW-MRCI/CBS	error
$(0,0^0,0)$	30782.4 (0.3)	—	
$(0,2^0,0)$	904.5 (0.3)	900.9	-3.6
$(0,4^0,0)$	1944.1 (1.1)	1930.5	-13.7
$(0,6^0,0)$	3049.9 (2.6)	3037.1	-12.8
$(0,8^0,0)$	4172.0 (3.7)	4155.2	-16.9
$(0,10^0,0)$	5298.9 (4.3)	5313.2	14.3
$(0,0^0,1)$	1292.4 (0.3)	1284.2	-8.2
$(0,2^0,1)$	2182.7 (0.5)	2197.8	15.1
$(0,4^0,1)$	3250.5 (1.6)	3243.9	-6.6
$(0,6^0,1)$	4365.1 (3.6)	4361.1	-4.0
$(0,8^0,1)$	5483.4 (5.0)	5494.1	10.7
$(0,10^0,1)$	6605.7 (5.1)	6617.0	11.3
$(0,2^0,2)$	3464.5 (0.8)	3488.2	23.7
$(0,4^0,2)$	4549.4 (4.3)	4553.2	3.8
$(1,2^0,0)$	3316.5 (0.9)	3335.8	19.2
$(1,4^0,0)$	4344.3 (3.1)	4347.5	3.2
$(1,6^0,0)$	5430.1 (5.5)	5406.3	-23.8
MUSE			11.9

^a Compared levels are reported relative to $T_0 = 30782.4$.

was motivated by concerns about possible convergence and root-flipping issues since the ground state can receive small weights using GDW in some regions.

The discrete variable representation (DVR) method^{17,18} was used to solve the vibrational Hamiltonian for zero total angular momentum in Jacobi coordinates. The potential was represented on a direct-product grid of potential optimized points^{19,20} including 70 points in each stretch coordinate and 60 for the bend (for a total of 294000 points). A potential ceiling was applied to the fitted surface at 25000 cm^{-1} . Level assignments were made by inspecting the structure of the calculated probability densities via 2D surface plots (e.g., Figure 2).

Calculated and experimental $J = 0$ band origins are compared in Table 1. The ground state of CDF is nearly 31000 cm^{-1} above the ground electronic state (experimentally, $T_0 = 30782.42 \text{ cm}^{-1}$). Since this study was limited to the \tilde{B} state to assess the GDW scheme, a value for T_0 has not yet been calculated as this will necessitate also fitting a ground-state PES and performing corresponding ground-state vibrational calculations. The barrier to linearity on the calculated \tilde{B} state surface is only 473 cm^{-1} , which is lower than the calculated zero-point energy (ZPE) of 2275 cm^{-1} . The minimum on the potential surface is at $\theta = 6.1^\circ$ in Jacobi coordinates (the D-C-F bond angle is 169.4°), while the maximum probability for the ground-state vibrational wave function occurs at $\theta = 3.5^\circ$. Note that for CHF, the increased ZPE (2807 cm^{-1}) results in a maximum angular probability at linear geometries ($\theta = 0.0^\circ$).

The vibrational levels computed for the GDW-MRCI PES are in excellent agreement with experimental results. For the 16 $J = 0$ band origins considered, including levels as high as 6606 cm^{-1} above the ZPE and more than 37000 cm^{-1} above the ground electronic state, the mean unsigned error (MUSE)

is only 11.9 cm^{-1} . Vibrational levels calculated using PESs constructed with the other ab initio schemes tested (fixed weights or equally weighted lower states) are in much poorer agreement with experiment ($\text{MUSE} > 40 \text{ cm}^{-1}$) and are not reported in detail here. The fixed weight PES suffered discontinuities in the MCSCF calculations (which are damped out somewhat by the subsequent MRCI calculations) that clearly impacted the accuracy of the vibrational calculations. Although these discontinuities only apparently impacted the tails of the vibrational wave functions for the levels studied here, calculations of certain other levels would be completely unreliable. For a given number of states included in a MCSCF calculation, the character of the highest state will tend to switch abruptly at certain values of the coordinates (corresponding to crossing an excluded state). If this state carries large weighting (such as with a fixed equal weights scheme), then discontinuities can occur in all of the states. With the GDW scheme, the highest states tend to receive negligible weight and thus can transition without significantly disrupting the state of interest. We note that the smooth evolution of the wave function produced by the GDW scheme is even more advantageous for trajectory studies where discontinuous gradients can be particularly problematic.

These results are very encouraging for the GDW scheme, having achieved predictive ab initio spectroscopic accuracy for a high-lying electronic state, without resorting to empirical adjustments. These results may be compared with ongoing spectroscopic calculations for other three atom systems with multireference character (HCO and HO_2), where we have observed significant ($\sim 10 \text{ cm}^{-1}$) shifts in calculated frequencies from effects such as core–valence and higher-order correlation. These effects were found to be important in a previous study as well.⁹ Since these and other small corrections were neglected in the present study, the level of agreement recorded may be somewhat fortuitous. Nevertheless, it is clear that the GDW scheme produces well-behaved and continuous potential energy surfaces with smoothly varying transitions between regions of differing electronic degeneracies and electronic structures and that the resulting potential energy surfaces can be of spectroscopic accuracy. The success of this method enables a possible future study, including vibrational energy levels for CHF and CDF with $J > 0$ and an exploration of the predissociation mechanism.

The experimental apparatus used in this work has been previously described in detail.^{21–29} Briefly, CHF (CDF) was produced using a pulsed discharge nozzle through a $\sim 1–2\%$ mixture of CH_2F_2 (CD_2F_2) in Ar. Specific rotational transitions in various bands of the $S_1 \leftarrow S_0$ ($\tilde{A} \leftarrow \tilde{X}$) system^{30,31} were excited by a tunable Nd:YAG pumped dye laser (Continuum P7010/Spectra Physics PDL-3). Approximately 300–400 ns later, a pulse from a second Nd:YAG pumped dye laser (Continuum NY-61/Lambda Physik Scanmate 2E), counter-propagating with the first, either excited specific transitions in the $S_2 \leftarrow S_1$ ($\tilde{B} \leftarrow \tilde{A}$) system or stimulated emission from $S_1 \rightarrow S_0$. Due to the very low fluorescence quantum yield of levels in the S_2 state as a consequence of fast nonradiative decay, a decrease in fluorescence was observed when the second laser was resonant with transitions in either the $S_2 \leftarrow S_1$ or $S_1 \rightarrow S_0$ system. However, the former transitions were lifetime-broadened

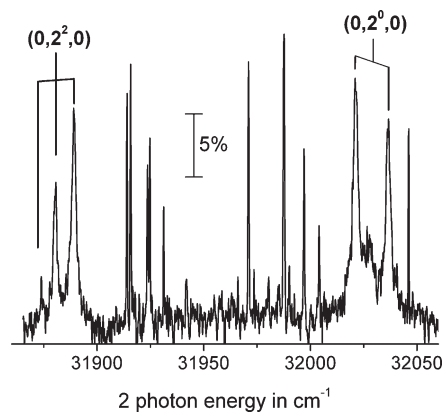


Figure 3. Rotationally resolved optical–optical double resonance (OODR) spectroscopy in the region of the $\tilde{B}(0,2,0)$ level of CHF. The narrower lines in this spectrum reflect downward (SEP) transitions to known rovibrational levels of the \tilde{X} state.

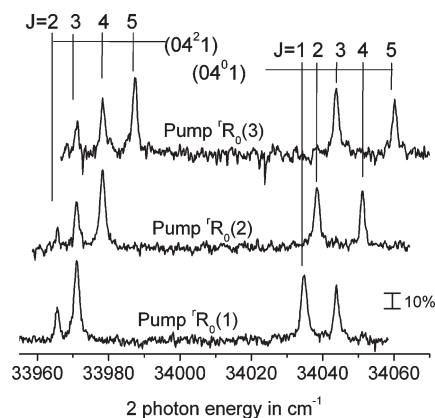


Figure 4. Rotationally resolved optical–optical double resonance (OODR) spectrum of the $\tilde{B}(0,4,1)$ level of CDF. This spectrum was obtained by pumping specific $^1R_0(J)$ lines (as noted in the figure) in the $(0,0,0)$ band of the $\tilde{A} \leftarrow \tilde{X}$ system.

while the latter were not, affording easy discrimination. Fluorescence depletions in excess of 50% were common for strongly predissociated $S_2 \leftarrow S_1$ transitions. The decrease in fluorescence caused by the second laser was measured using a dual gate boxcar system (Stanford Research Systems), where a portion of the fluorescence decay was integrated before and after the second laser pulse. The ratio of signal from each gate was recorded to remove the effect of significant shot-to-shot fluctuations in the signal. Typically, 10 shots were averaged at each step in wavelength. The wavelength of the pump laser was calibrated using the well-known $S_1 \leftarrow S_0$ spectroscopic constants, recalibrated to vacuum wavenumbers.^{30,32} The second laser was calibrated using optogalvanic spectroscopy in a Fe:Ne hollow cathode lamp.

Figures 3 and 4 display representative spectra of the $S_2 \leftarrow S_1$ bands of CHF (Figure 3) and CDF (Figure 4) which illustrate salient features of the spectroscopy of this system.

In Figures 3 and 4, the x-axis labels the energy above the vibrationless level of the \tilde{X} state (two-photon energy). As illustrated in Figures 3 and 4, the bands display the characteristic rotational structure of a c-type, bent-to-linear transition,

with rotational selection rules of $\Delta J = 0, \pm 1$ and $K_a - l = \pm 1$, where l is the vibrational angular momentum quantum number for the bending mode in the linear S_2 state and K_a is the associated rotational quantum number of the bent molecule in S_1 . Note that an additional selection rule governs transitions between each asymmetry doublet in S_1 and states of different parity in S_2 ; however, we do not resolve the asymmetry nor parity doublets in these experiments. By pumping different intermediate S_1 levels with $K_a = 0, 1$, and 2 in the progressions $2_0^n, 1_0^1 2_0^n$, and $2_0^2 3_0$, many S_2 levels with vibrational angular momentum, $l = 0-3$, could be accessed, with the restriction that even v contains only even l components and vice versa for odd v . Typically, spectra for a given S_2 level were obtained using several intermediate rotational (J) levels, as illustrated in Figure 4, and the observed rotational transitions were fit to a linear molecule rotational Hamiltonian using a nonlinear least-squares routine to derive the band origin and effective rotational constant.

AUTHOR INFORMATION

Corresponding Author:

*To whom correspondence should be addressed. E-mail: rdawes@sandia.gov. Phone: (925) 294-3404. Fax: (925) 294-2276 (R.D.); E-mail: scott.reid@mu.edu. Phone: (414) 288-7565. Fax: (414) 288-7066 (S.A.R.).

ACKNOWLEDGMENT R.D. and A.W.J. are supported by the Division of Chemical Sciences, Geosciences, and Biosciences, and the Office of Basic Energy Sciences, the U.S. Department of Energy; Sandia is a multiprogram laboratory operated by Sandia Corporation, a Lockheed Martin Company, for the National Nuclear Security Administration under Contract DE-AC04-94-AL85000. S.A.R. and S.H.K. acknowledge an Australian Academy of Science travel fellowship which allowed S.H.K. and S.A.R. to collaborate on the initial stages of this project. S.A.R. acknowledges the National Science Foundation (Grants CHE-0717960 and CHE-0353596) for support of this research. S.H.K. acknowledges the Australian Research Council for project funding (DP0665831).

REFERENCES

- Wang, X. G.; Carrington, T., Jr. A discrete variable representation method for studying the rovibrational quantum dynamics of molecules with more than three atoms. *J. Chem. Phys.* **2009**, *130*, 094101.
- Bowman, J. M.; Carrington, T., Jr.; Meyer, H. D. Variational quantum approaches for computing vibrational energies of polyatomic molecules. *Mol. Phys.* **2008**, *106*, 2145-2182.
- Huang, X. C.; Schwenke, D. W.; Lee, T. J. An Accurate Global Potential Energy Surface, Dipole Moment Surface, and Rovibrational Frequencies for NH_3 . *J. Chem. Phys.* **2008**, *129*, 214304.
- Marquardt, R.; Quack, M.; Thanopoulos, I.; Luckhaus, D. A Global Electric Dipole Function of Ammonia and Isotopomers in the Electronic Ground State. *J. Chem. Phys.* **2003**, *119*, 10724-10732.
- Brandao, J.; Rio, C. M. A.; Tennyson, J. A Modified Potential for HO_2 with Spectroscopic Accuracy. *J. Chem. Phys.* **2009**, *130*, 134309.
- Varandas, A. J. C.; Rodrigues, S. P. J. New Double Many-Body Expansion Potential Energy Surface for Ground State HCN from a Multiproperty Fit to Accurate Ab Initio Energies and Rovibrational Calculations. *J. Phys. Chem. A* **2007**, *111*, 4869-4870.
- Dawes, R.; Thompson, D. L.; Wagner, A. F.; Minkoff, M. Interpolating Moving Least-Squares Methods for Fitting Potential Energy Surfaces: A Strategy for Efficient Automatic Data Point Placement in High Dimensions. *J. Chem. Phys.* **2008**, *128*, 084107.
- Dawes, R.; Passalacqua, A.; Wagner, A. F.; Sewell, T. D.; Minkoff, M.; Thompson, D. L. Interpolating Moving Least-Squares Methods for Fitting Potential Energy Surfaces: Using Classical Trajectories to Explore Configuration Space. *J. Chem. Phys.* **2009**, *130*, 144107.
- Dawes, R.; Wagner, A. F.; Thompson, D. L. Ab Initio Wave-number Accurate Spectroscopy: $^1\text{CH}_2$ and HCN Vibrational Levels on Automatically Generated IMLS Potential Energy Surfaces. *J. Phys. Chem. A* **2009**, *113*, 4709-4721.
- Zhou, S.; Li, Z.; Xie, D.; Lin, S. Y.; Guo, H. An Ab Initio Global Potential-Energy Surface for $\text{NH}_2(A^2A')$ and Vibrational Spectrum of The Renner-Teller $A^2A'-X^2A''$ System. *J. Chem. Phys.* **2009**, *130*, 184307.
- Deskevich, M. P.; Nesbitt, D. J.; Werner, H. J. Dynamically Weighted Multiconfiguration Self-Consistent Field: Multistate Calculations For $\text{F} + \text{H}_2\text{O} \rightarrow \text{HF} + \text{OH}$ Reaction Paths. *J. Chem. Phys.* **2004**, *120*, 7281-7289.
- Werner, H.-J.; Knowles, P. J.; Lindh, R.; Manby, F. R.; Schütz, M.; et al. *MOLPRO*, version 2009.1; A Package of Ab Initio Programs; University College Cardiff Consultants Limited: Wales, U.K., 2009.
- Reactive Intermediate Chemistry*; Moss, R. A., Platz, M. S., Jones, M., Jr., Eds.; Wiley Interscience: Hoboken, NJ, 2004; Chapters 7-9.
- Herzberg, G.; Shoosmith, J. Spectrum and Structure of the Free Methylene Radical. *Nature* **1959**, *183*, 1801-1802.
- Fockenber, C.; Marr, A. J.; Sears, T. J.; Chang, B.-C. Near-Infrared High Resolution Diode Laser Spectrum of the $\text{CH}_2 b^1 B_1 \leftarrow a^1 A_1$ Transition. *J. Mol. Spectrosc.* **1998**, *187*, 119-125.
- Helgaker, T.; Jorgensen, P.; Olsen, J. *Molecular Electronic Structure Theory*; Wiley: New York, 2000.
- Light, J. C.; Carrington, T., Jr. Discrete-Variable Representations and Their Utilization. *Adv. Chem. Phys.* **2000**, *114*, 263-310.
- Lill, J. V.; Parker, G. A.; Light, J. C. Discrete-Variable Representations and Sudden Models in Quantum Scattering Theory. *Chem. Phys. Lett.* **1982**, *89*, 483-489.
- Wei, H.; Carrington, T., Jr. The Discrete Variable Representation of a Triatomic Hamiltonian in Bond Length-bond Angle Coordinates. *J. Chem. Phys.* **1992**, *97*, 3029-3037.
- Echave, J.; Clary, D. C. Potential Optimized Discrete Variable Representation. *Chem. Phys. Lett.* **1992**, *190*, 225-230.
- Fan, H.; Ionescu, I.; Annesley, C.; Reid, S. A. Lifetime Lengthening and the Renner-teller Effect in the $\text{HCF}(\tilde{A}^1A' \leftarrow \tilde{X}^1A')$ System. *Chem. Phys. Lett.* **2003**, *378*, 548-552.
- Deselnicu, M.; Tao, C.; Mukarakate, C.; Reid, S. A. Fluorescence Excitation and Emission Spectroscopy of the $\tilde{A}^1A' \leftarrow \tilde{X}^1A'$ System of CHBr . *J. Chem. Phys.* **2006**, *124*, 134302/11.
- Fan, H.; Mukarakate, C.; Deselnicu, M.; Tao, C.; Reid, S. A. Dispersed Fluorescence Spectroscopy of Jet-Cooled HCF and DCF: Vibrational Structure of the \tilde{X}^1A' State. *J. Chem. Phys.* **2005**, *123*, 014314/7.
- Ionescu, I.; Fan, H.; Ionescu, E.; Reid, S. A. Polarization Quantum Beat Spectroscopy of $\text{HCF}(\tilde{A}^1A')$. II. Renner-Teller and Spin-orbit Mixing in the Simplest Singlet Carbene. *J. Chem. Phys.* **2004**, *121*, 8874-8879.

- (25) Tao, C.; Deselnicu, M.; Mukarakate, C.; Reid, S. A. Electronic Spectroscopy of the $\tilde{A}^1A'' \leftrightarrow \tilde{X}^1A'$ System of CDBr. *J. Chem. Phys.* **2006**, *125*, 094305/9.
- (26) Tao, C.; Mukarakate, C.; Judge, R. H.; Reid, S. A. High Resolution Probe of Spin-Orbit Coupling and the Singlet-Triplet Gap in Chlorocarbene. *J. Chem. Phys.* **2008**, *128*, 171101/4.
- (27) Tao, C.; Mukarakate, C.; Reid, S. A. Fluorescence Excitation and Single Vibronic Level Emission Spectroscopy of the $\tilde{A}^1A'' \leftarrow \tilde{X}^1A'$ System of CHCl. *J. Chem. Phys.* **2006**, *124*, 224314/11.
- (28) Tao, C.; Mukarakate, C.; Terranova, Z.; Ebban, C.; Judge, R. H.; Reid, S. A. High Resolution Study of Spin-Orbit Mixing and the Singlet-Triplet Gap in Chlorocarbene: Stimulated Emission Pumping Spectroscopy of (CHCl)-Cl-35 and (CDCl)-Cl-35. *J. Chem. Phys.* **2008**, *129*, 104309/8.
- (29) Tao, C.; Reid, S. A.; Schmidt, T. W.; Kable, S. H. Observation of the Predissociated, Quasilinear $\tilde{B}(^1A')$ State of CHF by Optical-Optical Double Resonance. *J. Chem. Phys.* **2007**, *126*, 051105/4.
- (30) Fan, H.; Ionescu, I.; Annesley, C.; Cummins, J.; Bowers, M.; Xin, J.; Reid, S. A. On the Renner-Teller Effect and Barriers to Linearity and Dissociation in HCF (\tilde{A}^1A''). *J. Phys. Chem. A* **2004**, *108*, 3732-3738.
- (31) Schmidt, T. W.; Bacskay, G. B.; Kable, S. H. Characterization of the $\tilde{A}(^1A'')$ State of HCF by Laser Induced Fluorescence Spectroscopy. *J. Chem. Phys.* **1999**, *110*, 11277-11285.
- (32) Tao, C.; Deselnicu, M.; Fan, H.; Mukarakate, C.; Ionescu, I.; Reid, S. A. Electronic Spectroscopy of the $\tilde{A}^1A'' \leftarrow \tilde{X}^1A'$ System of CDF. *Phys. Chem. Chem. Phys.* **2006**, *8*, 707-713.